

# Measurements of the Mass and Full-Width of the $\eta_c$ Meson

J. Z. Bai<sup>1</sup>, Y. Ban<sup>9</sup>, J. G. Bian<sup>1</sup>, X. Cai<sup>1</sup>, J. F. Chang<sup>1</sup>, H. F. Chen<sup>16</sup>,  
H. S. Chen<sup>1</sup>, Jie Chen<sup>8</sup>, J. C. Chen<sup>1</sup>, Y. B. Chen<sup>1</sup>, S. P. Chi<sup>1</sup>, Y. P. Chu<sup>1</sup>,  
X. Z. Cui<sup>1</sup>, Y. M. Dai<sup>7</sup>, Y. S. Dai<sup>19</sup>, L. Y. Dong<sup>1</sup>, S. X. Du<sup>18</sup>, Z. Z. Du<sup>1</sup>,  
W. Dunwoodie<sup>13</sup>, J. Fang<sup>1</sup>, S. S. Fang<sup>1</sup>, C. D. Fu<sup>1</sup>, H. Y. Fu<sup>1</sup>, L. P. Fu<sup>6</sup>,  
C. S. Gao<sup>1</sup>, M. L. Gao<sup>1</sup>, Y. N. Gao<sup>14</sup>, M. Y. Gong<sup>1</sup>, W. X. Gong<sup>1</sup>, S. D. Gu<sup>1</sup>,  
Y. N. Guo<sup>1</sup>, Y. Q. Guo<sup>1</sup>, Z. J. Guo<sup>2</sup>, S. W. Han<sup>1</sup>, F. A. Harris<sup>15</sup>, J. He<sup>1</sup>,  
K. L. He<sup>1</sup>, M. He<sup>10</sup>, X. He<sup>1</sup>, Y. K. Heng<sup>1</sup>, T. Hong<sup>1</sup>, H. M. Hu<sup>1</sup>, T. Hu<sup>1</sup>,  
G. S. Huang<sup>1</sup>, L. Huang<sup>6</sup>, X. P. Huang<sup>1</sup>, J. M. Izen<sup>17</sup>, X. B. Ji<sup>1</sup>,  
C. H. Jiang<sup>1</sup>, X. S. Jiang<sup>1</sup>, D. P. Jin<sup>1</sup>, S. Jin<sup>1</sup>, Y. Jin<sup>1</sup>, B. D. Jones<sup>17</sup>,  
Z. J. Ke<sup>1</sup>, D. Kong<sup>15</sup>, Y. F. Lai<sup>1</sup>, F. Li<sup>1</sup>, G. Li<sup>1</sup>, H. H. Li<sup>5</sup>, J. Li<sup>1</sup>, J. C. Li<sup>1</sup>,  
K. Li<sup>6</sup>, Q. J. Li<sup>1</sup>, R. B. Li<sup>1</sup>, R. Y. Li<sup>1</sup>, W. Li<sup>1</sup>, W. G. Li<sup>1</sup>, X. Q. Li<sup>8</sup>,  
X. S. Li<sup>14</sup>, C. F. Liu<sup>18</sup>, C. X. Liu<sup>1</sup>, Fang Liu<sup>16</sup>, F. Liu<sup>5</sup>, H. M. Liu<sup>1</sup>,  
J. B. Liu<sup>1</sup>, J. P. Liu<sup>18</sup>, R. G. Liu<sup>1</sup>, Y. Liu<sup>1</sup>, Z. A. Liu<sup>1</sup>, Z. X. Liu<sup>1</sup>,  
X. C. Lou<sup>17</sup>, G. R. Lu<sup>4</sup>, F. Lu<sup>1</sup>, H. J. Lu<sup>16</sup>, J. G. Lu<sup>1</sup>, Z. J. Lu<sup>1</sup>, X. L. Luo<sup>1</sup>,  
E. C. Ma<sup>1</sup>, F. C. Ma<sup>7</sup>, J. M. Ma<sup>1</sup>, R. Malchow<sup>3</sup>, Z. P. Mao<sup>1</sup>, X. C. Meng<sup>1</sup>,  
X. H. Mo<sup>2</sup>, J. Nie<sup>1</sup>, Z. D. Nie<sup>1</sup>, S. L. Olsen<sup>15</sup>, D. Paluselli<sup>15</sup>, H. P. Peng<sup>16</sup>,  
N. D. Qi<sup>1</sup>, C. D. Qian<sup>11</sup>, J. F. Qiu<sup>1</sup>, G. Rong<sup>1</sup>, D. L. Shen<sup>1</sup>, H. Shen<sup>1</sup>,  
X. Y. Shen<sup>1</sup>, H. Y. Sheng<sup>1</sup>, F. Shi<sup>1</sup>, L. W. Song<sup>1</sup>, H. S. Sun<sup>1</sup>, S. S. Sun<sup>16</sup>,  
Y. Z. Sun<sup>1</sup>, Z. J. Sun<sup>1</sup>, S. Q. Tang<sup>1</sup>, X. Tang<sup>1</sup>, D. Tian<sup>1</sup>, Y. R. Tian<sup>14</sup>,  
W. Toki<sup>3</sup>, G. L. Tong<sup>1</sup>, G. S. Varner<sup>15</sup>, J. Wang<sup>1</sup>, J. Z. Wang<sup>1</sup>, L. Wang<sup>1</sup>,  
L. S. Wang<sup>1</sup>, M. Wang<sup>1</sup>, Meng Wang<sup>1</sup>, P. Wang<sup>1</sup>, P. L. Wang<sup>1</sup>,  
W. F. Wang<sup>1</sup>, Y. F. Wang<sup>1</sup>, Zhe Wang<sup>1</sup>, Z. Wang<sup>1</sup>, Zheng Wang<sup>1</sup>,  
Z. Y. Wang<sup>2</sup>, C. L. Wei<sup>1</sup>, N. Wu<sup>1</sup>, X. M. Xia<sup>1</sup>, X. X. Xie<sup>1</sup>, G. F. Xu<sup>1</sup>,  
Y. Xu<sup>1</sup>, S. T. Xue<sup>1</sup>, M. L. Yan<sup>16</sup>, W. B. Yan<sup>1</sup>, G. A. Yang<sup>1</sup>, H. X. Yang<sup>14</sup>,  
J. Yang<sup>16</sup>, S. D. Yang<sup>1</sup>, M. H. Ye<sup>2</sup>, Y. X. Ye<sup>16</sup>, J. Ying<sup>9</sup>, C. S. Yu<sup>1</sup>,  
G. W. Yu<sup>1</sup>, C. Z. Yuan<sup>1</sup>, J. M. Yuan<sup>1</sup>, Y. Yuan<sup>1</sup>, Q. Yue<sup>1</sup>, S. L. Zang<sup>1</sup>,  
Y. Zeng<sup>6</sup>, B. X. Zhang<sup>1</sup>, B. Y. Zhang<sup>1</sup>, C. C. Zhang<sup>1</sup>, D. H. Zhang<sup>1</sup>,  
H. Y. Zhang<sup>1</sup>, J. Zhang<sup>1</sup>, J. M. Zhang<sup>4</sup>, J. W. Zhang<sup>1</sup>, L. S. Zhang<sup>1</sup>,  
Q. J. Zhang<sup>1</sup>, S. Q. Zhang<sup>1</sup>, X. Y. Zhang<sup>10</sup>, Y. J. Zhang<sup>9</sup>, Yiyun Zhang<sup>12</sup>,  
Y. Y. Zhang<sup>1</sup>, Z. P. Zhang<sup>16</sup>, D. X. Zhao<sup>1</sup>, Jiawei Zhao<sup>16</sup>, J. W. Zhao<sup>1</sup>,  
P. P. Zhao<sup>1</sup>, W. R. Zhao<sup>1</sup>, Y. B. Zhao<sup>1</sup>, Z. G. Zhao<sup>1†</sup>, J. P. Zheng<sup>1</sup>,  
L. S. Zheng<sup>1</sup>, Z. P. Zheng<sup>1</sup>, X. C. Zhong<sup>1</sup>, B. Q. Zhou<sup>1</sup>, G. M. Zhou<sup>1</sup>,  
L. Zhou<sup>1</sup>, N. F. Zhou<sup>1</sup>, K. J. Zhu<sup>1</sup>, Q. M. Zhu<sup>1</sup>, Yingchun Zhu<sup>1</sup>, Y. C. Zhu<sup>1</sup>,  
Y. S. Zhu<sup>1</sup>, Z. A. Zhu<sup>1</sup>, B. A. Zhuang<sup>1</sup>, B. S. Zou<sup>1</sup>.

(The BES Collaboration)

<sup>1</sup> Institute of High Energy Physics, Beijing 100039, People's Republic of China

<sup>2</sup> China Center of Advanced Science and Technology, Beijing 100080, People's

Republic of China

<sup>3</sup> Colorado State University, Fort Collins, Colorado 80523

<sup>4</sup> Henan Normal University, Xinxiang 453002, People's Republic of China

<sup>5</sup> Huazhong Normal University, Wuhan 430079, People's Republic of China

<sup>6</sup> Hunan University, Changsha 410082, People's Republic of China

<sup>7</sup> Liaoning University, Shenyang 110036, People's Republic of China

<sup>8</sup> Nankai University, Tianjin 300071, People's Republic of China

<sup>9</sup> Peking University, Beijing 100871, People's Republic of China

<sup>10</sup> Shandong University, Jinan 250100, People's Republic of China

<sup>11</sup> Shanghai Jiaotong University, Shanghai 200030, People's Republic of China

<sup>12</sup> Sichuan University, Chengdu 610064, People's Republic of China

<sup>13</sup> Stanford Linear Accelerator Center, Stanford, California 94309

<sup>14</sup> Tsinghua University, Beijing 100084, People's Republic of China

<sup>15</sup> University of Hawaii, Honolulu, Hawaii 96822

<sup>16</sup> University of Science and Technology of China, Hefei 230026, People's Republic of China

<sup>17</sup> University of Texas at Dallas, Richardson, Texas 75083-0688

<sup>18</sup> Wuhan University, Wuhan 430072, People's Republic of China

<sup>19</sup> Zhejiang University, Hangzhou 310028, People's Republic of China

<sup>†</sup> Visiting professor to University of Michigan, Ann Arbor, MI 48109, USA

---

## Abstract

In a sample of 58 million  $J/\psi$  events collected with the BES II detector, the process  $J/\psi \rightarrow \gamma\eta_c$  is observed in five different decay channels:  $\gamma K^+ K^- \pi^+ \pi^-$ ,  $\gamma \pi^+ \pi^- \pi^+ \pi^-$ ,  $\gamma K^\pm K_S^0 \pi^\mp$  (with  $K_S^0 \rightarrow \pi^+ \pi^-$ ),  $\gamma \phi \phi$  (with  $\phi \rightarrow K^+ K^-$ ) and  $\gamma p \bar{p}$ . From a combined fit of all five channels, we determine the mass and full-width of  $\eta_c$  to be  $m_{\eta_c} = 2977.5 \pm 1.0$  (stat.)  $\pm 1.2$  (syst.) MeV/ $c^2$  and  $\Gamma_{\eta_c} = 17.0 \pm 3.7$  (stat.)  $\pm 7.4$  (syst.) MeV/ $c^2$ .

*PACS:* 13.25.Gv, 14.40.Gx, 13.40.Hq

---

Since 1980, numerous efforts have been made to determine the mass and full width of the  $\eta_c$  [1–11]. However, from a theoretical point of view, the accuracies of these experimental measurements are still not sufficient. For instance, in order to calculate the strength of the spin-spin interaction term in non-relativistic potential models, it is necessary to know precisely the mass difference between the  $J/\psi(1^{--})$  and  $\eta_c(0^{-+})$ . While the mass of the  $J/\psi$  is determined with high accuracy to be  $3096.88 \pm 0.04$  MeV/ $c^2$ , the  $\eta_c$  mass is measured with much less accuracy to be  $2979.7 \pm 1.5$  MeV/ $c^2$ , an average by the Particle Data Group (PDG) [12] of 10 measurements with an internal confidence level of only 0.001. Different measurements of the full width of the  $\eta_c$  also have poor internal consistency. The PDG [12] determines an average value for the  $\eta_c$  full width of  $16.0^{+3.6}_{-3.2}$  MeV/ $c^2$  from six experiments, whose experimental results vary from 7 MeV/ $c^2$  to 27 MeV/ $c^2$ , with large errors. Such an accuracy is inadequate for some studies of charmonium physics [13] and additional, more precise measurements of both  $m_{\eta_c}$  and  $\Gamma_{\eta_c}$  are needed.

The  $\eta_c$  mass and width have been measured previously by the BES collaboration with data samples of 3.79 million  $\psi(2S)$  events [9] and 7.8 million  $J/\psi$  events [11] collected with the BES I detector [14]. In the latter sample, the process  $J/\psi \rightarrow \gamma\eta_c$  was observed in five different  $\eta_c$  decay channels:  $K^+K^-\pi^+\pi^-$ ,  $\pi^+\pi^-\pi^+\pi^-$ ,  $K^\pm K_S^0 \pi^\mp$  (with  $K_S^0 \rightarrow \pi^+\pi^-$ ),  $\phi\phi$  (with  $\phi \rightarrow K^+K^-$ ) and  $K^+K^-\pi^0$ , and the mass of the  $\eta_c$  was determined to be  $2976.6 \pm 2.9$  (stat.)  $\pm 1.3$  (syst.) MeV/ $c^2$ . Combined with the results from  $\psi(2S) \rightarrow \gamma\eta_c$ , the mass and the full width of  $\eta_c$  were determined to be  $m_{\eta_c} = 2976.3 \pm 2.3$  (stat.)  $\pm 1.2$  (syst.) MeV/ $c^2$  and  $\Gamma_{\eta_c} = 11.0 \pm 8.1$  (stat.)  $\pm 4.1$  (syst.) MeV/ $c^2$ .

In this paper we present results with much higher statistics using a recent sample of 58 million  $J/\psi$  events obtained with the upgraded BESII detector [15]. The upgrade from BES I to BES II includes the replacement of the inner drift chamber with a straw-tube vertex chamber (VC), composed of 12 tracking layers arranged around a beryllium beam pipe and with a spatial resolution of about 90  $\mu\text{m}$ ; a new barrel time-of-flight counter (BTOF) with a time resolution of 180 ps; and a new main drift chamber (MDC), which has 10 tracking layers providing a  $dE/dx$  resolution of  $\sigma_{dE/dx} = 8.4\%$  and a momentum resolution of  $\sigma_p/p = 1.7\% \sqrt{1+p^2}$  ( $p$  in GeV) for charged tracks. These upgrades augment the pre-existing calorimeter and muon tracking systems. The barrel shower counter (BSC), which covers 80% of  $4\pi$  solid angle, has an energy resolution of  $\sigma_E/E = 22\%/\sqrt{E}$  ( $E$  in GeV) and a spatial resolution of 7.9 mrad in  $\phi$  and 2.3 cm in  $z$ . The  $\mu$  identification system consists of three double layers of proportional tubes interspersed in the iron flux return of the magnet. They provide coordinate measurements along the muon trajectories with resolutions of 3 cm and 5.5 cm in  $\phi$  and  $z$ , respectively.

The  $\eta_c$  mass and width are measured using the reactions  $J/\psi \rightarrow \gamma\eta_c$ ;  $\eta_c \rightarrow$

$K^+K^-\pi^+\pi^-$ ,  $\pi^+\pi^-\pi^+\pi^-$ ,  $K^\pm K_S^0\pi^\mp$  (with  $K_S^0 \rightarrow \pi^+\pi^-$ ),  $\phi\phi$  (with  $\phi \rightarrow K^+K^-$ ) and  $p\bar{p}$ . Event selection criteria for each channel are described in detail in our previous papers [16,17,18]. Here we repeat only the essential information and emphasize those considerations that are unique to the  $m_{\eta_c}$  and  $\Gamma_{\eta_c}$  measurements.

Candidate events are required to have the correct number of charged tracks for a given hypothesis. Each track must be well fit to a helix in the polar angle range  $|\cos\theta| < 0.84$  and have a transverse momentum above 60 MeV/c. For the decay channels  $J/\psi \rightarrow \gamma K^+K^-\pi^+\pi^-$ ,  $J/\psi \rightarrow \gamma\pi^+\pi^-\pi^+\pi^-$ ,  $J/\psi \rightarrow \gamma K^\pm\pi^\mp\pi^+\pi^-$  and  $J/\psi \rightarrow \gamma p\bar{p}$ , at least one photon with energy  $E_\gamma > 30$  MeV is required in the barrel shower counter

Events are kinematically fitted with four constraints (4C) to the hypotheses:  $J/\psi \rightarrow \gamma K^+K^-\pi^+\pi^-$ ,  $J/\psi \rightarrow \gamma\pi^+\pi^-\pi^+\pi^-$ ,  $J/\psi \rightarrow \gamma K^\pm\pi^\mp\pi^+\pi^-$ , and  $J/\psi \rightarrow \gamma p\bar{p}$ . A one-constraint(1C) fit is performed for the  $J/\psi \rightarrow \gamma_{miss}K^+K^-K^+K^-$  hypothesis, where  $\gamma_{miss}$  indicates that this photon is not detected. Events with a  $\chi^2$  less than 40.0 for a particular channel are selected.

In order to remove backgrounds from non-radiative decay channels, all selected events are subjected to a kinematic fit with four constraints to the hypotheses:  $J/\psi \rightarrow K^+K^-\pi^+\pi^-$ ,  $J/\psi \rightarrow \pi^+\pi^-\pi^+\pi^-$  and  $J/\psi \rightarrow K^\pm\pi^\mp\pi^+\pi^-$ . Backgrounds from the  $J/\psi$  peak are removed by requiring that  $\chi^2(J/\psi \rightarrow K^+K^-\pi^+\pi^-) > 20.0$  (for  $K^+K^-\pi^+\pi^-$ );  $\chi^2(J/\psi \rightarrow \pi^+\pi^-\pi^+\pi^-) > 10.0$  (for  $\pi^+\pi^-\pi^+\pi^-$ ) and  $\chi^2(J/\psi \rightarrow K^\pm\pi^\mp\pi^+\pi^-) > 10.0$  (for  $K^\pm K_S^0\pi^\mp$ ). For the  $J/\psi \rightarrow \gamma p\bar{p}$  channel, we require that the opening angle of the two charged tracks is smaller than  $179^\circ$ . A detailed Monte Carlo simulation shows that these cuts, referred to below as the  $J/\psi$  veto, do not distort the invariant mass distributions around the  $\eta_c$  signal peak.

Two additional variables are used to reject events with wrong final state assignments. The first variable,  $|U_{miss}| = |E_{miss} - P_{miss}|$ , is used to reject events with multi-photons and misidentified charged particles. Here,  $E_{miss}$  and  $P_{miss}$  are, respectively, the missing energy and momentum calculated using measured quantities for charged tracks. A second variable,  $P_{t\gamma}^2 = 4|P_{miss}|^2 \sin^2(\theta_{t\gamma}/2)$ , where  $\theta_{t\gamma}$  is the angle between the missing momentum and the photon direction, is used to reduce backgrounds from  $\pi^0$ 's. The specific values of the selection requirements for these two kinematic variables are summarized in Table 1. Additional requirements to remove backgrounds from a few specific channels are summarized in Table 2.

For  $J/\psi \rightarrow \gamma\pi^+\pi^-\pi^+\pi^-$  candidate events with more than one  $\gamma$ , we suppress  $\pi^0$  background by requiring that  $|M(\gamma_1\gamma_2) - M(\pi^0)| > 60$  MeV/c<sup>2</sup> if  $\vec{P}_{miss}$  is in the same plane as the two photons  $\gamma_1$  and  $\gamma_2$ , i.e.  $\hat{P}_{miss} \cdot (\hat{r}_{\gamma_1} \times \hat{r}_{\gamma_2}) < 0.15$ . Here,  $\hat{P}_{miss}$  is the unit vector of the missing momentum for all charged tracks;

Table 1

Cuts imposed on  $|U_{miss}|$  and  $P_{t\gamma}^2$  for event selection.

mode ( $J/\psi \rightarrow \gamma X$ )	$ U_{miss} $ ( $\text{GeV}/c^2$ )	$P_{t\gamma}^2$ [ $(\text{GeV}/c)^2$ ]
$\gamma K^+ K^- \pi^+ \pi^-$	$< 0.15$	$< 0.002$
$\gamma \pi^+ \pi^- \pi^+ \pi^-$	$< 0.10$	$< 0.0015$
$\gamma K^\pm K_S^0 \pi^\mp$ ( $\gamma K^\pm \pi^\mp \pi^+ \pi^-$ )	–	$< 0.003$
$\gamma p \bar{p}$	$< 0.15$	$< 0.003$

Table 2

Cuts to remove backgrounds from specific channels.

mode ( $J/\psi \rightarrow \gamma X$ )	cut	background
$\gamma K^+ K^- \pi^+ \pi^-$	$ M_{\pi^+ \pi^- \pi^0} - M_\omega  > 40 \text{ MeV}/c^2$	$J/\psi \rightarrow \omega K^+ K^-$
$\gamma K^+ K^- \pi^+ \pi^-$	$ M_{K^+ K^-} - M_\phi  > 20 \text{ MeV}/c^2$	$J/\psi \rightarrow \phi \pi^+ \pi^-$
$\gamma \pi^+ \pi^- \pi^+ \pi^-$	$ M_{\pi^+ \pi^- \pi^0} - M_\omega  > 40 \text{ MeV}/c^2$	$J/\psi \rightarrow \omega \pi^+ \pi^-$
$\gamma \pi^+ \pi^- \pi^+ \pi^-$	$ M_{\pi^+ \pi^-} - M_{K_S^0}  > 25 \text{ MeV}/c^2$	$J/\psi \rightarrow \gamma K_S^0 K_S^0$

$r_{\hat{\gamma}_1}$  and  $r_{\hat{\gamma}_2}$  are unit vectors for the  $\gamma_1$  and  $\gamma_2$  directions determined from the BSC; and  $M(\gamma_1 \gamma_2)$  is the invariant mass of  $\gamma_1 \gamma_2$ . When we calculate  $M(\gamma_1 \gamma_2)$ , it is assumed that the missing particle decays to  $\gamma_1$  and  $\gamma_2$ , and  $M(\gamma_1 \gamma_2)$  can be obtained by using  $P_{miss}$  and the angles between  $\vec{P}_{miss}$  and the  $\gamma$  direction. The advantage of this technique is that it uses the momenta of charged tracks measured by the MDC, which has good momentum resolution, and is independent of the photon energy measurement. For  $J/\psi \rightarrow \gamma K^+ K^- \pi^+ \pi^-$ ,  $\gamma K^\pm K_S^0 \pi^\mp$ , and  $\gamma p \bar{p}$ , we require that  $|M(\gamma_1 \gamma_2) - M(\pi^0)| > 50 \text{ MeV}/c^2$  when  $\vec{P}_{miss} \cdot (r_{\hat{\gamma}_1} \times r_{\hat{\gamma}_2}) < 0.14$ .

For the  $K^\pm K_S^0 \pi^\mp$  (with  $K_S^0 \rightarrow \pi^+ \pi^-$ ) channel, the  $\pi^+ \pi^-$  invariant mass for the  $K_S^0$  candidate is required to be within  $25 \text{ MeV}/c^2$  of the  $K_S^0$  mass. For the  $\phi\phi$  (with  $\phi \rightarrow K^+ K^-$ ) channel, the invariant masses of both candidate  $\phi$ 's, corresponding to  $K^+ K^-$  pairs, are required to be within  $20 \text{ MeV}/c^2$  of the  $\phi$  mass.

After the event selection, the invariant mass spectra for the individual decay modes are obtained, as shown in Fig. 1. An unbinned maximum likelihood fit using MINUIT [19] is performed for all five channels simultaneously, with the fitting function for a given channel  $i$  given by

$$f_i(m) = a_i [BW(M, \Gamma, m) \otimes GS(m, \sigma_i)] \times EFF_i(m) + (1 - a_i) BG_i(m),$$

where  $M$  and  $\Gamma$  are the mass and width of the  $\eta_c$ , respectively,  $\sigma_i$  is the mass resolution in the  $\eta_c$  region,  $BW$  is a Breit-Wigner function describing the  $\eta_c$  signal,  $EFF_i$  is an efficiency correction function, and  $BG_i$  is a second-order

polynomial function describing the background shape. In order to include the experimental resolution, the  $BW$  function is folded with a Gaussian resolution function  $GS$  with the resolution  $\sigma_i$  fixed at a value determined from the Monte Carlo simulation. The parameters  $M$  and  $\Gamma$  and the coefficients of the polynomial function,  $a_i$ , are determined from the fit. The log likelihood function for the channel  $i$  is given by

$$S_i = -\ln L_i = -\ln\left(\prod_{j=1}^{N_i^{\text{event}}} f_i(m_j)\right),$$

where  $N_i^{\text{event}}$  is the total number of events. The overall log likelihood function,

$$S = \sum_{i=1}^5 S_i,$$

is minimized to obtain the fitting results from the five channels simultaneously. The fit result is shown in Fig. 1, and the fitted  $\eta_c$  mass and width are determined to be  $m_{\eta_c} = 2977.5 \pm 1.0 \text{ MeV}/c^2$  and  $\Gamma_{\eta_c} = 17.0 \pm 3.7 \text{ MeV}/c^2$ . The background in Fig. 1(b),(d) and (e) can also be fitted with a linear polynomial function, with results that are almost the same.

Systematic errors in determining the  $\eta_c$  mass and width originate mainly from the mass-scale calibration, background shape, fitting range, difference between data and Monte Carlo simulation,  $J/\psi$  veto, and uncertainties associated with the mass resolution. We use 1.5 million  $\psi(2S)$  data collected during the  $J/\psi$  run to check the mass-scale calibration. The measured  $\chi_{c2}$  mass is  $3555.2 \pm 1.4 \text{ MeV}/c^2$  from decays  $\psi(2S) \rightarrow \gamma\pi^+\pi^-\pi^+\pi^-$  and  $3560.2 \pm 6.0 \text{ MeV}/c^2$  from decays  $\psi(2S) \rightarrow \gamma K^+K^-\pi^+\pi^-$ , respectively. The combined weighted average is  $m_{\chi_{c2}} = 3555.5 \pm 1.4 \text{ MeV}/c^2$ , a difference of  $0.7 \pm 1.4 \text{ MeV}/c^2$  from the world average obtained by the PDG [12]. In addition, we measured masses of the  $K_s^0$ ,  $\phi$  and  $\Lambda$  from the 58 million  $J/\psi$  data sample to check the mass-scale calibration. Results of the masses and mass differences with PDG values [12] are given in Table 3. The systematic error on the overall mass scale is estimated to be  $0.8 \text{ MeV}/c^2$ .

Table 3

Comparison of  $K_s^0$ ,  $\phi$  and  $\Lambda$  mass peak positions.

	$K_s^0$ (MeV/ $c^2$ )	$\phi$ (MeV/ $c^2$ )	$\Lambda$ (MeV/ $c^2$ )
our measurements	$496.9 \pm 0.1$	$1019.6 \pm 0.1$	$1115.3 \pm 0.1$
PDG values	$497.67 \pm 0.03$	$1019.417 \pm 0.014$	$1115.683 \pm 0.006$
$\Delta M$	$-0.8 \pm 0.1$	$0.2 \pm 0.1$	$-0.4 \pm 0.1$

Table 4 summarizes all contributions to the systematic error of the mass and full-width of the  $\eta_c$ . The effect of the background shape is studied by using a third-order polynomial function instead of a second-order one. The upper

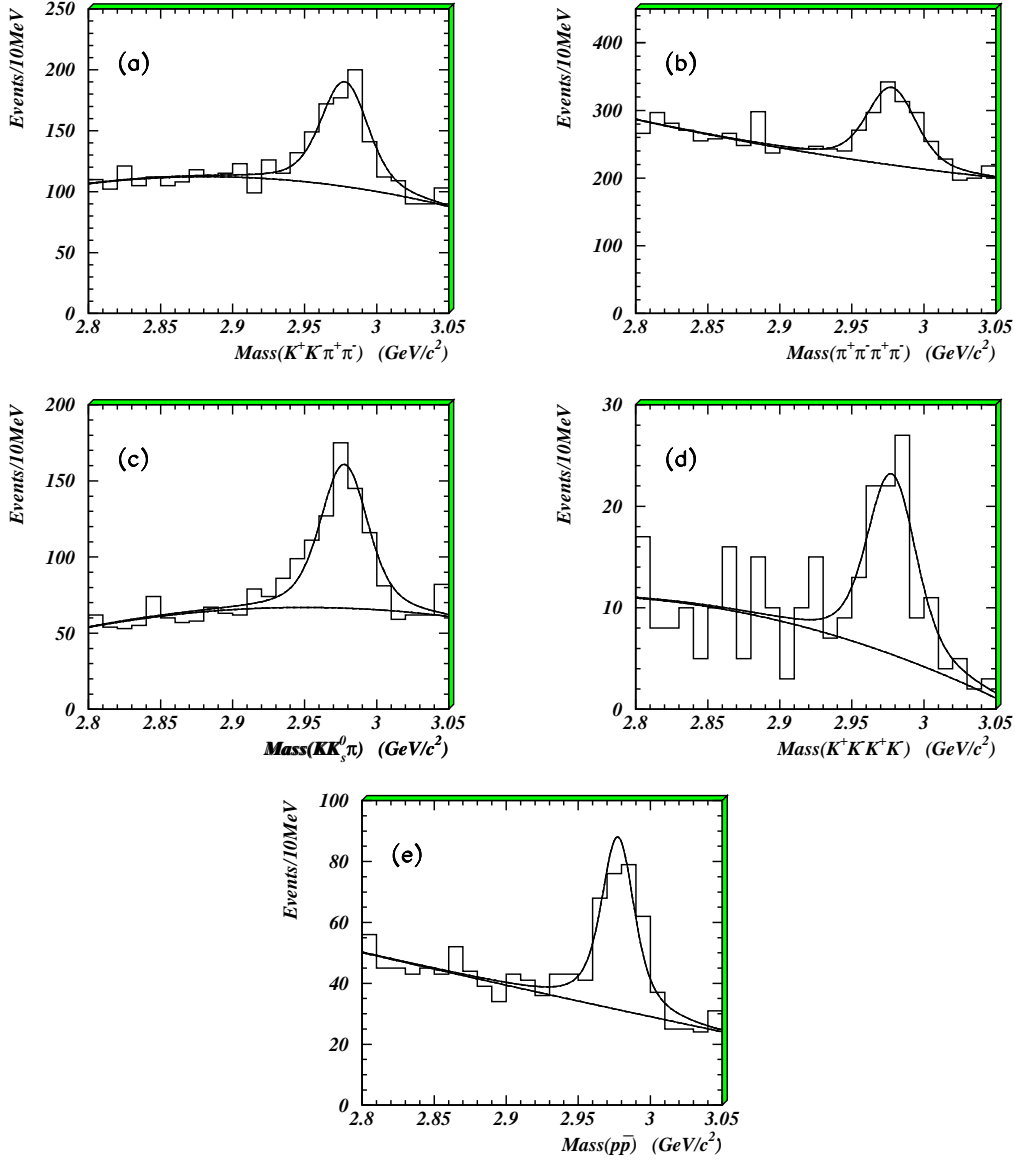


Fig. 1. The invariant mass distributions in the  $\eta_c$  region for channels (a)  $m_{K^+K^-\pi^+\pi^-}$ , (b)  $m_{\pi^+\pi^-\pi^+\pi^-}$ , (c)  $m_{K^\pm K_S^0 \pi^\mp}$ , (d)  $m_{\phi\phi}$  and (e)  $m_{p\bar{p}}$ .

fitting bound is checked by changing it from 3.05 to 3.07  $\text{GeV}/c^2$ , and the  $J/\psi$  veto is removed from the event selection. Contributions from differences of the detection efficiency between data and Monte Carlo simulation, as well as uncertainties of the detector mass resolution, are also listed in Table 4. Assuming no correlations among the above factors, the total systematic error on the mass and width are determined to be 1.2  $\text{MeV}/c^2$  and 7.4  $\text{MeV}/c^2$ , respectively, by a quadratic sum of all contributions.

In summary, we used 58 million  $J/\psi$  events collected by the BES II detector to measure the mass and full width of the  $\eta_c$  in five different decay modes. They are determined to be  $m_{\eta_c} = 2977.5 \pm 1.0$  (stat.)  $\pm 1.2$  (syst.)  $\text{MeV}/c^2$

and  $\Gamma_{\eta_c} = 17.0 \pm 3.7$  (stat.)  $\pm 7.4$  (syst.) MeV/ $c^2$ . Figure 2 shows the BES results together with previously reported measurements. It can be seen that the  $\eta_c$  mass and width measurement from BES II are in good agreement with the PDG averages.

Table 4  
Sources of systematic errors.

sources	error on mass (MeV/ $c^2$ )	error on width (MeV/ $c^2$ )
mass scale calibration	0.8	
background shape	0.0	3.6
fitting range	0.3	2.2
detection efficiency difference: data vs. MC	0.5	0.3
$J/\psi$ veto	0.7	5.6
uncertainties of experimental mass resolution	0.0	2.4
total systematic error	1.2	7.4

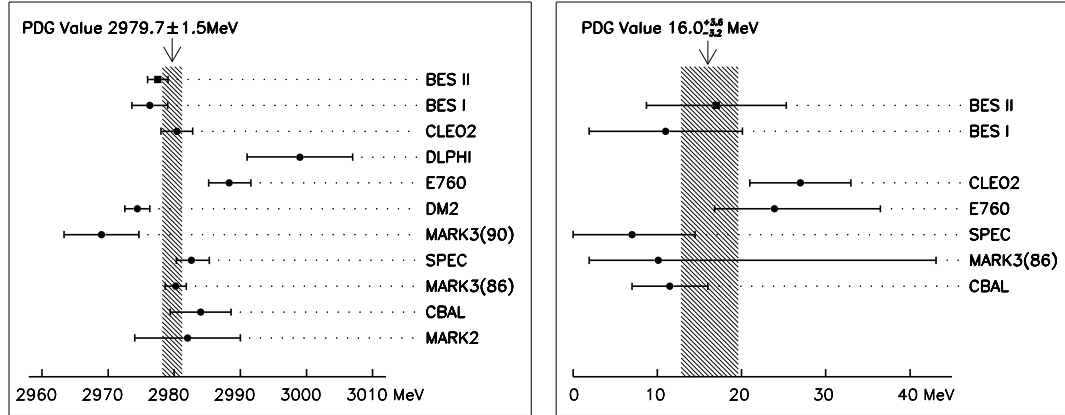


Fig. 2. Mass and full-width measurements of the  $\eta_c$  meson.

The BES collaboration expresses their thanks for the hard efforts of the staff of BEPC and the computing center at the Institute of High Energy Physics, Beijing. This work is supported in part by the National Natural Science Foundation of China under contracts Nos. 19991480,10175060 and the Chinese Academy of Sciences under contract No. KJ 95T-03(IHEP); and by the Department of Energy under Contract Nos. DE-FG03-93ER40788 (Colorado State University), DE-AC03-76SF00515 (SLAC), DE-FG03-94ER40833 (U Hawaii), DE-FG03-95ER40925 (UT Dallas).



## References

- [1] T.M. Himel *et al.*, Phys. Rev. Lett. **45**, 1146 (1980).
- [2] J. Gaiser *et al.*, (Crystal Ball Collaboration), Phys. Rev. **D 34**, 711 (1986).
- [3] K.M. Baltrusaitis *et al.* (MARK III Collaboration), Phys. Rev. **D 33** , 629 (1986).
- [4] C. Berger *et al.*, Phys. Lett. **B 167**, 191 (1987).
- [5] Z. Bai *et al.* (MARK III Collaboration), Phys. Rev. Lett. **65**, 1309 (1990).
- [6] D. Bisello *et al.* (DM2 Collaboration), Nucl. Phys. **B 350** , 1 (1991).
- [7] T.A. Armstrong *et al.*, Phys. Rev. **D 52**, 4839 (1995).
- [8] P. Abreu *et al.* (DELPHI Collaboration), Phys. Lett. **B 441**, 479 (1998).
- [9] J.Z. Bai *et al.* (BES Collaboration), Phys. Rev. **D 60**, 072001 (1999).
- [10] G. Brandenburg *et al.* (CLEO Collaboration), Phys. Rev. Lett. **85**, 3095 (2000).
- [11] J.Z. Bai *et al.* (BES Collaboration), Phys. Rev. **D 62**, 072001 (2000).
- [12] Particle Data Group, Phys. Rev. **D 66**, 01001-719 (2002).
- [13] Yu-Ping Kuang, Phys. Rev. **D 65**, 094024 (2002).
- [14] J.Z. Bai *et al.* (BES Collaboration), Nucl. Instr. Meth., **A344** 319 (1994).
- [15] J.Z. Bai *et al.* (BES Collaboration), Nucl. Instr. Meth., **A458** 627 (2001).
- [16] J.Z. Bai *et al.* (BES Collaboration), Phys. Lett. **B 472**, 200 (2000).
- [17] J.Z. Bai *et al.* (BES Collaboration), Phys. Lett. **B 472**, 207 (2000).
- [18] J.Z. Bai *et al.* (BES Collaboration), Phys. Lett. **B 476**, 25 (2000).
- [19] F.James, CERN Program Library Long Writeup D506.